

# Impact of Carrier Systems on the Interactions of Coenzyme Q<sub>10</sub> with Model Lipid Membranes

Ajda Ota<sup>1</sup> · Marjeta Šentjura<sup>2</sup> · Marjan Bele<sup>3</sup> · Pegi Ahlin Grabnar<sup>4</sup> · Nataša Poklar Ulrih<sup>1</sup>

Received: 20 May 2015 / Accepted: 5 October 2015 / Published online: 16 October 2015  
© Springer Science+Business Media New York 2015

**Abstract** We investigated the influence of carrier systems for different commercially available water-soluble formulations for coenzyme Q<sub>10</sub> on structural changes of model lipid membranes formed by 1,2-dipalmitoyl-*sn*-glycero-3-phosphocholine and by a mixture of phosphatidylcholine and sphingomyelin (2.4:1). Structural changes in the membranes were measured using fluorescence anisotropy, electron paramagnetic resonance, and differential scanning calorimetry. Two fluorophores and two spin probes were used to monitor membrane characteristics close to the water-lipid interface and in the middle of the bilayer of the model lipid membranes. Different water-soluble carrier systems were tested. These data show that different systems can facilitate penetration of CoQ<sub>10</sub> in the lipid membranes, where an increase in the lipid order parameter was observed. In addition, water soluble CoQ<sub>10</sub> formulations better protect lipids from oxidation in liposome solution. With the exception of the carriers in an

emulsified formulation of CoQ<sub>10</sub>, those in the other samples did not have any significant effects on membrane fluidity.

**Keywords** Coenzyme Q<sub>10</sub> · Fluorescence spectroscopy · Electron paramagnetic resonance · Model membranes · Membrane fluidity · Differential scanning calorimetry

## Introduction

Coenzyme Q<sub>10</sub> (2,3-dimethoxy-5-methyl-6-multiprenyl-1,4-benzoquinone), also known as ubiquinone or ubidecarenone, is a lipid-soluble compound found in the cells of many organisms. CoQ<sub>10</sub> is involved in a variety of essential cellular processes, such as transmembrane electron transport systems in the respiratory chain of mitochondria, and as a stabilising agent in cell membranes [1]. As bioavailability of CoQ<sub>10</sub> in humans is relatively low due to its lipophilic nature and large molecular mass [2], several formulations have been developed to improve its bioavailability [3]. These approaches have included micro-encapsulation of CoQ<sub>10</sub> using different mixtures of gum arabic, maltodextrin, and modified starches [4], nanoparticles with incorporated CoQ<sub>10</sub> [5, 6], self-emulsifying drug-delivery systems [7], formulations of redispersible dry emulsions [8], and cyclodextrin complexes [9], to name just a few. Coenzyme Q<sub>10</sub> is now widely used as a food supplement and these forms of CoQ<sub>10</sub> have allowed fortification of several aqueous products [10]. Recently the bio-accessibility of micellarized form of CoQ<sub>10</sub> in processed meat products fortified with CoQ<sub>10</sub> was investigated [11].

Encapsulation provides protection of active compounds against oxidation and light-induced reactions and can be used to increase their solubility. By preventing reactions with components in the food system in which they are present,

---

**Electronic supplementary material** The online version of this article (doi:10.1007/s11483-015-9417-0) contains supplementary material, which is available to authorized users.

---

✉ Nataša Poklar Ulrih  
natasa.poklar@bf.uni-lj.si

<sup>1</sup> Biotechnical Faculty, University of Ljubljana, Jamnikarjeva 101, SI-1000 Ljubljana, Slovenia

<sup>2</sup> Institute “Jožef Stefan”, Jamova cesta 39, SI-1000 Ljubljana, Slovenia

<sup>3</sup> National Institute of Chemistry Slovenia, Hajdrihova 19, SI-1001 Ljubljana, Slovenia

<sup>4</sup> Faculty of Pharmacy, University of Ljubljana, Aškerčeva cesta 7, SI-1000 Ljubljana, Slovenia

encapsulation allows such active compounds to be used in the formulation of several fortified and functional foods [12, 13].

Carbohydrates are the most common carrier materials, such as hydrolysed and emulsifying starches and gums. These are used extensively as supports for the encapsulation of food ingredients. Several methods have been developed to modify starch, which require the use of chemicals and enzymes. Carriers based on different modified starches and their blends with other components have been successfully used for encapsulation of food ingredients and drugs [14–18].

Given the importance and variety of the functions of CoQ<sub>10</sub> in cell membranes, it is important to understand the influence of its carrier systems on membrane-lipid interactions, such as for different formulations of water-soluble CoQ<sub>10</sub>. Model lipid membranes are particularly suitable for investigations into the permeability of drugs and drug delivery systems, and they allow the use of various spectroscopic techniques to study the biophysical interactions. Studies in cell culture and in vivo have shown that drug–lipid interactions have significant roles in the pharmacokinetic properties of drugs, such as in their transport, distribution, and accumulation, and that they ultimately influence the efficacy of drugs. The properties of carriers used in drug delivery systems have been shown to influence the drug interactions with cells and tissue. To develop an efficient drug carrier system, a better understanding of the mechanisms behind the drug delivery system uptake is necessary [19].

The effects on the structural properties of model lipid membranes of four water-soluble CoQ<sub>10</sub> formulations that are used in food supplements were investigated. These formulations contained the following four different mixtures of carriers: (i) an emulsified preparation of glycerol in combination with polyglycerol fatty-acid ester (PGE), soybean lecithin, and fatty-acid triglyceride (sample A); (ii) encapsulated in pregelatinised starch combined with gum arabic and lactose (sample B); (iii) with starch sodium octenylsuccinate and dextrin and glycerol (sample C); and (iv) with  $\beta$ -cyclodextrin as the sole carrier (sample D). The analyses included a combination of fluorescence anisotropy, electron paramagnetic resonance (EPR) spectroscopy, and differential scanning calorimetry (DSC). Two fluorophores and two spin labels were used to monitor the membrane characteristics, with one of each targeting the water–lipid interface, and the other two targeting the middle of the bilayer.

## Materials and Methods

### Materials

The phospholipids phosphatidylcholine (PC; from egg), sphingomyelin (SM; from egg) and 1,2-dipalmitoyl-sn-glycero-3-phosphocholine (DPPC) were from Avanti Polar

Lipids (USA). The fluorophores 1,6-diphenyl-1,3,5-hexatriene (DPH) and N,N,N-trimethyl-4-(6-phenyl-1,3,5-hexatrien-1-yl)phenylammonium p-toluenesulphonate (TMA-DPH), and soybean lecithin and HEPES were from Sigma Aldrich Chemical Company (USA). BODIPY® 581/591 C<sub>11</sub> (4,4-difluoro-5-(4-phenyl-1,3-butadienyl)-4-bora-3a,4a-diaza-s-indacene-3-undecanoic acid) was from Invitrogen Molecular Probes (USA). CuCl<sub>2</sub>, dextrin, glycerin and gum arabic were from Kemika (Croatia),  $\beta$ -cyclodextrin was from Jiangsu Fengyunu Biotechnology Co., Ltd. (Japan), pregelatinised starch was from Huzhou Zhanwang Pharmaceutical Co., Ltd. (China), and starch sodium octenylsuccinate was from Dequin Sanfu Food Co., Ltd. (China). PGE was a kind gift from Zhengzhou Honest Food Co., Ltd. Fatty-acid triglyceride was from Cognis (Germany), and organic solvents were from Merck (Germany). The spin label methyl esters of doxyl palmitic acid with the doxyl group on carbon 5 [MeFASL(10,3)] and on carbon 13 [MeFASL(2,11)] of the alkyl chain (counting from the methyl group) were synthesised by Prof. Slavko Pečar at the Faculty of Pharmacy, University of Ljubljana, Slovenia.

The four commercially available water-soluble CoQ<sub>10</sub> formulations used were:

- (i) Sample A: an emulsified preparation containing 10.8 %  $\pm$ 0.2 % CoQ<sub>10</sub>, 54.5 % glycerol, 12 % PGE, 5 % fatty-acid triglyceride and 3 % soybean lecithin;
- (ii) Sample B: containing 13.2 %  $\pm$ 0.2 % CoQ<sub>10</sub> encapsulated in 30 % pregelatinised starch, 24 % gum arabic and 22 % lactose;
- (iii) Sample C: containing 42.0 %  $\pm$ 0.2 % CoQ<sub>10</sub>, 40 % starch sodium octenyl succinate, 15 % dextrin and 3 % glycerol;
- (iv) Sample D: containing 14.9 %  $\pm$ 0.2 % CoQ<sub>10</sub> and 75 %  $\beta$ -cyclodextrin.

## Methods

### Preparation of Liposomes

Multilamellar liposomes from DPPC or from PC and SM at a molar ratio of 2.4:1 (PC/SM) were prepared using the thin layer method [20]. These multilamellar liposomes (final lipid concentration, 5 mg/mL) were prepared by transferring 1 mL DPPC stock solution (10 mg/mL in chloroform) or 725  $\mu$ L PC plus 275.5  $\mu$ L SM stock solutions (10 mg/mL in chloroform; respectively) into rotary flasks. The solvents were completely evaporated under reduced pressure (17 mbar), to provide a thin phospholipid film in the flasks. These lipid films were hydrated by adding 2 mL 10 mM HEPES (buffered to pH 7.0 with NaOH), and the mixtures were heated to above the phase transition temperature of the phospholipids in the

liposome preparations and shaken for 2 h; i.e., 45 °C for the formation of DPPC multilamellar liposomes, and 40 °C for the formation of PC/SM multilamellar liposomes [21].

Small unilamellar liposomes/vesicles (SUVs) were prepared from these multilamellar liposomes before each measurement. The multilamellar liposomes were sonicated using a high intensity ultrasonic processor (Sonics Vibra Cell VCX 750) in an ice-cold bath for 15 min, as continuous repeating 10-s on-off intervals. The SUVs formed were used for fluorescence anisotropy and EPR spectroscopy, while the multilamellar liposomes were used for DSC measurements. An in-vitro assay for quantitative determination of phospholipids was used for verification of the phospholipid concentrations (Phospholipid C; Wako Pure Chemical Industries, Ltd., Japan).

### Scanning Electronic Microscopy

The surfaces of samples were examined using field-emission scanning electron microscopy (SEM; Supra 35 VP; Carl Zeiss) at an accelerating voltage of 1 kV. Before imaging, the samples were mounted on a sample holder using double-sided conductive carbon tape.

### Size Distribution, Polydispersity Index and Zeta Potential Measurements

Dispersions were characterized by average particle diameter, polydispersity index (PDI) and  $\zeta$ -potential (ZP). The average particle size and PDI were determined by photon correlation spectroscopy with a Zetasizer Nano ZS (Malvern Instruments, Worcestershire, UK) at 25 °C and a scattering angle of 173°. Zeta potential measurements were performed using a Zetasizer Nano ZS by electrophoretic laser Doppler velocimetry at 25 °C. The zeta potentials were calculated from the electrophoretic mobility by applying the Smoluchowski equation. All measurements were performed in a folded capillary cell (DTS 1060 C, Malvern Instruments). For data analysis, the viscosity (0.88 mPa s) and the refractive index (1.33) of distilled water at 25 °C were used.

### Fluorescence Emission Anisotropy

The fluorescence anisotropy measurements were performed in a 10-mm-path-length cuvette using a fluorescence spectrophotometer (Cary Eclipse; Varian, Australia) at 25 and 45 °C. Aliquots of the SUVs (50  $\mu$ L) were labelled with the fluorophores DPH or TMA-DPH (1 and 2 mM stock solutions in dimethylsulphoxide, respectively) and diluted to 2.5 mL with 10 mM HEPES, pH 7.0. The final lipid concentration was 0.1 mg/mL, with 1  $\mu$ M DPH or 2  $\mu$ M TMA-DPH. Samples of the water-soluble CoQ<sub>10</sub> formulations and the carriers in each of these four formulations were dissolved in ultrapure

water, while the pure CoQ<sub>10</sub> solution was prepared in 99 % ethanol. Sample solutions were added to SUV suspensions labelled with DPH or TMA-DPH. This allowed investigation of the effects of these formulations and their components on these model membranes, as the ratio  $n_{\text{Lig}}/n_{\text{Lip}}$ , with  $n_{\text{Lig}}$  moles of CoQ<sub>10</sub> formulation to  $n_{\text{Lip}}$  moles of lipid in the range from 0 to 1.8. These data were expressed as the anisotropy ( $r$ ), which indicates the fluorescence anisotropy of DPH or TMA-DPH in the presence of the water-soluble CoQ<sub>10</sub> formulations or their components, with regard to the ultrapure water and ethanol used as the controls. The fluorescence anisotropy was measured at an excitation wavelength of 358 nm, with the excitation polariser oriented vertically, while the vertical and horizontal components of the polarised light were recorded through the monochromator at 410 nm. The anisotropy was calculated using the built-in software of the instrument, as in Eq. (1):

$$r = I_{HH} - GI_{HV} / (I_{HH} + 2GI_{HV}). \quad (1)$$

The value of the G-factor, and the ratio of the sensitivities of the detection system for vertically ( $I_{HV}$ ) and horizontally polarised light ( $I_{HH}$ ), were determined separately for each sample. From the anisotropy, the lipid-order parameter was calculated according to Eq. (2) [22]:

$$S = \left[ 1 - 2(r/r_0) + 5(r/r_0)^2 \right]^{1/2} - 1 + r/r_0 / 2(r/r_0), \quad (2)$$

where  $r_0$  is the fluorescence anisotropy of DPH in the absence of any rotational motion of the probe. The fluidity was defined as the reciprocal of the lipid-order parameter. The theoretical  $r_0$  was 0.4, while the experimental  $r_0$  was between 0.362 and 0.394 [22]. In the calculations, the experimental values of  $r_0 = 0.370$  for DPH and  $r_0 = 0.369$  for TMA-DPH in DPPC at 5 °C were used [23].

### Electron Paramagnetic Resonance

The SUVs were first spin-labelled with either MeFASL(10,3), which was used to monitor the membrane properties close to the water–lipid interface, or MeFASL(2,11), which was used to monitor the properties in the middle of the membranes. For this, 35  $\mu$ L aliquots of  $10^{-4}$  M solutions of the spin probes in ethanol were dried in test-tubes, to obtain a uniform thin film of the probe on the walls of the test-tubes. Then 50  $\mu$ L aliquots of the liposome suspensions (5 mg lipid/mL) were added. The suspensions were mixed for 10 min, and then 28.7  $\mu$ L of the water-soluble CoQ<sub>10</sub> formulation dissolved in ultrapure water (5 mg/mL CoQ<sub>10</sub>) was added. The same volume of ultrapure water was used as the control. The mixtures were vortexed for 5 min, transferred to 1-mm capillary tubes (Euroglas, Slovenia), and measured in an X-band EPR spectrometer (Elexsys 500; Bruker, Germany) across the temperature range of 10 to

50 °C, at 5 °C intervals. The molar ratio of lipid to CoQ<sub>10</sub> was 2:1.

The empirical correlation time ( $\tau_{emp}$ ) was calculated from the spectra using Eq. (3) [24]:

$$\tau_{emp} = k\Delta H \left[ (h_0/h_{-1})^{1/2} - 1 \right], \quad (3)$$

where  $k$  is a constant typical for the spin probe, as  $5.9387 \times 10^{-11} \text{ mT}^{-1}$  for MeFASL(10,3) and MeFASL(2,11) [25], and the line width ( $\Delta H$ , in mT) and the height of the mid-field ( $h_0$ ) and high-field ( $h_{-1}$ ) lines were obtained from the EPR spectra. This provided rough estimates of the ordering and dynamics of the spin-probe motion and the changes caused by the incorporation of the CoQ<sub>10</sub> or carriers into the membrane in each sample. A short empirical correlation time indicated low ordering of the phospholipid acyl chains, fast motion of the nitroxide group of the spin probe, and consequently high average membrane fluidity.

As described previously [26, 27], the EPR data measured directly from the spectra provide information about the average fluidity characteristics of the membrane in the vicinity of the probe, without taking into account that the membrane is heterogeneous, as it is composed of regions with different fluidity characteristics (e.g., lateral membrane heterogeneity, inner and outer leaflets of the membrane, nitroxide group close to the polar head groups, different depths in the membrane layers). Therefore, for a more precise description of the membrane characteristics, computer simulation of the EPR spectra was performed with the EPRSIM WIZ 6.2.2. programme (<http://www.ijss.si/ijss/dept/epr>). This takes into account that the experimental EPR spectrum is a superposition of several spectral components with sets of parameters that reflect the spin-probe motion in different membrane environments [28, 29].

Each spectral component was described with a set of spectral parameters that included: an order parameter ( $S$ ), the rotational correlation time ( $\tau_c$ ), an additional broadening constant ( $W$ ), the polarity correction factor of the hyperfine coupling tensor ( $p_A$ ) and of the  $g$  tensor ( $p_g$ ), and the fraction of each spectral component ( $d$ ). The order parameter,  $S$ , describes the orientation order of the spin-probe nitroxide group and depends on the ordering of the surrounding phospholipid acyl chains.  $S$  varies from 1 for perfectly ordered membranes, to 0 for isotropic distribution of the molecules. The rotational correlation time,  $\tau_c$ , describes the dynamics of the rotational motion of the spin probe, which is influenced by the motion of the acyl chains of the surrounding lipids. This is short for fast motion of a spin probe and long in slow motion regions, as typical for viscous fluids. The additional broadening constant, or the line-width correction,  $W$ , arises from the unresolved hydrogen super-hyperfine interactions and contributions from other

paramagnetic impurities (e.g., oxygen, external magnetic field inhomogeneities). The polarity correction factors  $p_g$  and  $p_A$  arise from the polarity of the environment of the spin-probe nitroxide group. The line-shape of the EPR spectra was defined by the relative proportion of each spectral component,  $d$ , which describes the relative amount of the spin probe with a particular motional mode, and this depends on the distribution of the spin probe molecules between the co-existing regions with different fluidity characteristics. According to published results on similar system [30] we suppose that the spin probes are equally distributed between the co-existing regions. Therefore the fraction of spin probes in the co-existing regions should reflect the real fraction of the regions with different fluidity characteristics. It should be stressed that the lateral motion of the spin probe within the membrane is slow on the time scale of EPR measurements [31]. Therefore, each spectral component describes only the properties of the nearest surroundings of the spin probe at the nanometer scale, as the sum of all of the membrane regions with the same properties.

#### Differential Scanning Calorimetry

Gel-to-liquid crystalline phase transitions of the DPPC lipid were monitored using a Nano DSC series III DSC system (Calorimetry Science, Provo, USA). The phase transitions of the multilamellar liposomes prepared from DPPC (0.5 mg/mL) were monitored in the presence of the water-soluble CoQ<sub>10</sub> formulations and their components (molar ratio, 1:1 for CoQ<sub>10</sub> to lipid; i.e., with the same amount of each component in the sample). The measurements were performed as previously described by Ota et al. [32].

#### Evaluation of Inhibition of Lipid Peroxidation

To determine the antioxidative potential of the water-soluble formulations of CoQ<sub>10</sub>, the BODIPY® 581/591 C<sub>11</sub> lipophilic fluorogenic probe was used. This assay is based on the sensitivity of this BODIPY® 581/591 C<sub>11</sub> assay to oxidation by radicals formed from lipid hydroperoxides [33].

Aliquots of the SUVs were labelled with the fluorogenic probe BODIPY® 581/591 C<sub>11</sub> (2 mM stock solution in dimethylsulphoxide) and diluted to 2.5 mL with 10 mM HEPES, pH 7.0. The final concentrations were 1 mg/mL lipid and 1 μM BODIPY® 581/591 C<sub>11</sub>. The samples were incubated for 15 min at 25 °C. Peroxidation of the PC SUVs was induced by addition of 20 μL 1 mM CuCl<sub>2</sub>. The fluorescence emission from the BODIPY® 581/591 C<sub>11</sub> was measured at an excitation wavelength of 500 nm and emission wavelength of 520 nm.

## Results and Discussion

### Scanning Electronic Microscopy

The SEM micrographs of the powdered samples (samples B, C, D) showed typical spray-dried particles in the size range from 5 to 100  $\mu\text{m}$ . Sample B showed spherical particles, while the particles in samples C and D were more irregular in shape (Fig. 1).

### Size Distribution, Polydispersity Index and Zeta Potential Measurements

Studied samples exhibit a broad range of sizes from 50 to 2300 nm in water suspension. Water suspensions of samples B, C and D are more heterogeneous compared to water suspension of sample A (PDI = 0.12). All studied CoQ<sub>10</sub> formulations have comparable zeta potential between –30 and –40 mV. Results are presented in Table 1.

### Fluorescence Anisotropy

The changes in the fluorescence anisotropy of the DPH and TMA-DPH were measured to define the ordering parameter of the lipid bilayers of the DPPC and PC/SM (2.4:1) SUVs. DPH is a non-polar fluorophore and is used to monitor changes in the middle of the membrane bilayer. TMA-DPH is an amphiphilic compound and is used to probe membrane properties more towards the lipid-head-group region [34]. The anisotropy is greatest when the lipid environment is in the gel crystalline state, lowest in the liquid-disordered state, and intermediate in the liquid-ordered state [35]. The lipid order parameter ( $S$ ) was calculated from the anisotropy values.

The changes in  $S$  after the titration of the SUVs constituted from DPPC or PC/SM in the ethanol solution of crystalline CoQ<sub>10</sub> at 10 mg/mL are shown in Fig. 2. Ethanol alone slightly decreased the anisotropy of both DPH and TMA-DPH. The slight decrease in the order parameter  $S$  at 25 °C was observed in the upper part of the membranes, closer to the polar head-groups of the DPPC SUVs, as measured with TMA-DPH (Fig. 2a).

**Table 1** Size distribution, polydispersity index (PDI) and zeta potential measurements of CoQ<sub>10</sub> formulations. Measurements were performed in duplicates

Sample	Size (nm)	PDI	Zeta potential (mV)
A	49.8 ± 0.3	0.12 ± 0.01	–40.0
B	815 ± 4	0.6 ± 0.1	–37.3
C	2280 ± 50	0.49 ± 0.03	–26.0
D	541 ± 19	0.51 ± 0.06	–30.9

When the DPPC SUVs were titrated with CoQ<sub>10</sub>, there were no significant changes in the membrane order parameter  $S$  using DPH at 25 °C, probably because at this temperature the membranes of the SUVs are in the gel phase and CoQ<sub>10</sub> cannot penetrate into the membranes. At 45 °C, where the SUVs are in the liquid crystalline phase, there was an increase in the order parameter  $S$  (Fig. 2a), which indicated penetration of CoQ<sub>10</sub> into the membranes. These data are in agreement with the findings of Jemiola-Rzeminska et al. [36], who observed a small change induced by CoQ<sub>10</sub> at lower temperatures. At higher concentrations, CoQ<sub>10</sub> was probably located in the midplane layer of the membrane, below the DPH penetrated region. Above the phase transition temperature, CoQ<sub>10</sub> penetrates into the membranes and orders the membrane-lipid side chains [36].

For the PC/SM SUVs, there was an increase in the order parameter  $S$  of DPH at 25 °C as well as at 45 °C, which indicated changes in the membrane interior detected by DPH, while changes in the upper parts of the membranes were not as pronounced (Fig. 2b).

Figures 3 and 4 show the changes in the lipid order parameter  $S$  after the titration of the SUVs constituted from DPPC and from PC/SM, respectively, with the water suspensions of the CoQ<sub>10</sub> formulations containing 2 mg/mL CoQ<sub>10</sub> in the presence of DPH and TMA-DPH.

For the DPPC SUVs (Fig. 3), when the emulsified water-soluble CoQ<sub>10</sub> formulation (sample A) was used with the DPH fluorophore at 25 °C there was an ordering of the acyl chains (i.e., increased  $S$ ; Fig. 3a), while for the carriers alone in this formulation (glycerol, soybean lecithin, PGE emulsifier, fatty-acid triglycerides) there was a significant decrease in the

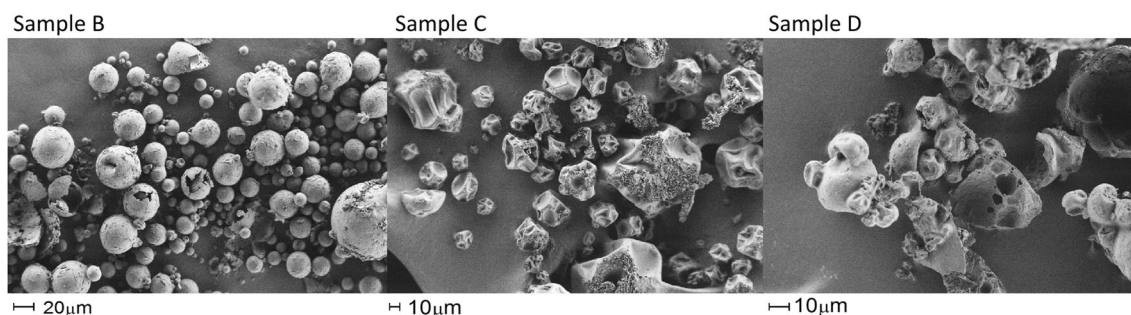
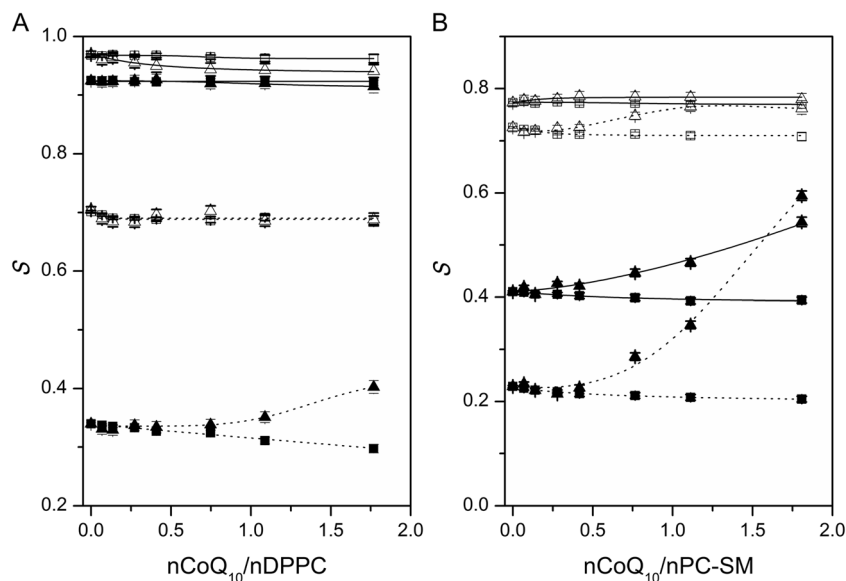


**Fig. 1** SEM images of the powdered water-soluble CoQ<sub>10</sub> formulations

**Fig. 2** Changes in the lipid order parameter  $S$  after titration of DPPC SUVs (a) and PC/SM SUVs (b) with the ethanol solution of CoQ<sub>10</sub> (10 mg/mL;  $\blacktriangle$ ); solid line, 25 °C; dotted line, 45 °C. Fluorophores: DPH, filled symbols; TMA-DPH, open symbols. Absolute ethanol was used for the control ( $\square$ ). Error bars represent standard error from two independent experiments



order parameter  $S$  (Fig. 3a). With the addition of the CoQ<sub>10</sub> encapsulated in pregelatinised starch, gum arabic and lactose (sample B) and with CoQ<sub>10</sub> with  $\beta$ -cyclodextrin (sample D) there were small decreases in the order parameter  $S$  with the DPH fluorophore at 25 °C (Fig. 3a). However, above the DPPC phase-transition temperature (at 45 °C; Fig. 3b) there was an ordering when these water soluble formulations were added. This ordering was greatest with CoQ<sub>10</sub> encapsulated in pregelatinised starch, gum arabic and lactose (sample B), followed by sample C, where starch sodium octenylsuccinate was the main carrier; this effect was then less pronounced for sample D, as CoQ<sub>10</sub> in  $\beta$ -cyclodextrin, and finally less again for the emulsified CoQ<sub>10</sub> (sample A). It is likely that in these cases the carrier mixtures facilitate CoQ<sub>10</sub> penetration into the membrane. The easier penetration of CoQ<sub>10</sub> into the DPPC bilayer might be a result of better dispersion of the CoQ<sub>10</sub> formulation in the lipid suspension compared to crystalline CoQ<sub>10</sub>, which provides it with better contact with the SUV membranes.

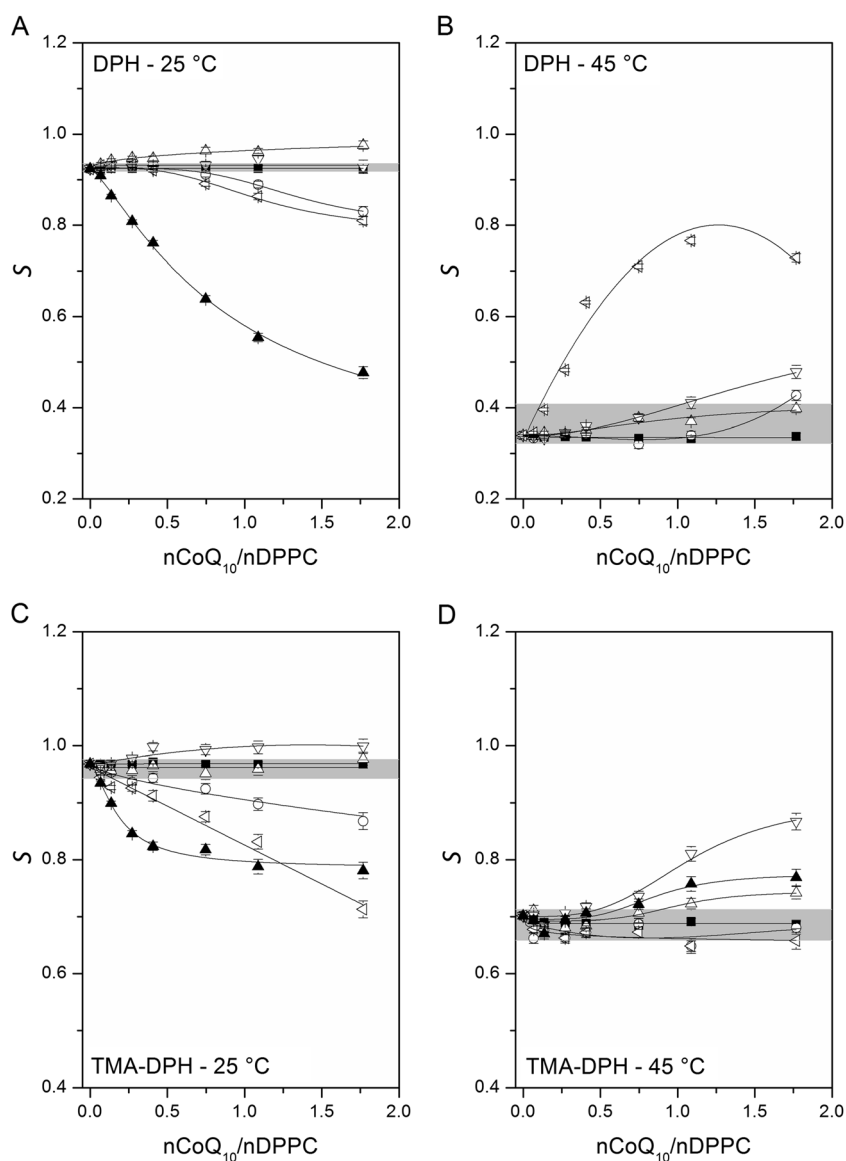
The changes in the lipid order parameter  $S$  after titration of the PC/SM SUVs with the water suspensions of the CoQ<sub>10</sub> formulations containing 2 mg/mL CoQ<sub>10</sub> in the presence of DPH and TMA-DPH are shown in Fig. 4. At 25 °C, addition of water suspensions of samples A, B and C resulted in increases in the order parameter  $S$  detected by DPH, which suggests the incorporation of the CoQ<sub>10</sub> into the lipid bilayer. The significant increase in the ordering of the DPPC acyl chains at 45 °C that was seen with CoQ<sub>10</sub> encapsulated in the pregelatinised starch, gum arabic and lactose mixture (Fig. 3b, sample B) was also seen for the PC/SM SUVs (Fig. 4b, sample B). In these PC/SM SUVs, there were also increases in the order parameter  $S$  for samples A, C and D. For the  $\beta$ -cyclodextrin complex and the PC/SM SUVs (Fig. 4b, sample D), the increase was

probably caused by the partial displacement of CoQ<sub>10</sub> from the  $\beta$ -cyclodextrin cavity and its accommodation in the lipid bilayer. The rate of this transition is likely to be dependent on the stability constant of the complex [37]. Here, the increases in the ordering of the acyl chains of the PC/SM SUVs with the water suspensions of the CoQ<sub>10</sub> formulations were generally greater than those seen for the DPPC SUVs, at both 25 and 45 °C (except for sample B at 45 °C), which suggests that the lipid composition affects this interaction.

When the various effects of the carriers alone were taken into account, there were generally no significant changes at 25 and 45 °C for the DPPC and PC/SM SUVs (Figs. 3 and 4 show the grey areas within which these remained), with the exception of the carriers of sample A with DPH at 25 °C (Figs. 3a and 4a). Sample A contained glycerol, soybean lecithin, the PGE emulsifier, and fatty-acid triglyceride, and alone (i.e., without the addition of CoQ<sub>10</sub>) it caused a significant decrease in the lipid order parameter  $S$  defined by the DPH integrated into both the DPPC SUVs and the PC/SM SUVs at 25 °C (Figs. 3a and 4a). Based on the composition of the carrier system in sample A, this can be expected. This combination of the PGE emulsifier, glycerol and soybean lecithin results in a decrease in the membrane ordering. These data confirm that for the rest of the systems, the changes detected in the lipid bilayer were the results of the CoQ<sub>10</sub> incorporation into the membrane, and are not effects of the carrier system used.

The changes in membrane fluidity observed after addition of the water-soluble CoQ<sub>10</sub> formulations indicate that water-soluble formulations enable CoQ<sub>10</sub> penetration into the membrane lipid bilayer, where increases in the ordering and decreases in the dynamics of the phospholipid acyl chains were observed.

**Fig. 3** Changes in the lipid order parameter  $S$  after titration of DPPC SUVs with the fluoroprobes DPH (a, b) and TMA-DPH (c, d) at 25 °C (a, c) and 45 °C (b, d). Data are shown for the water-soluble CoQ<sub>10</sub> formulations with the CoQ<sub>10</sub> concentration of 2 mg/mL, as sample A ( $\triangle$ ), sample B ( $\square$ ), sample C ( $\nabla$ ), and sample D ( $\circ$ ). For clarity, where the changes in the lipid order parameter  $S$  as a result of the carriers alone were located within the grey area, the data are not shown, while the carriers alone for Sample A are shown (a, c, d;  $\blacktriangle$ ). Ultra pure water was used as the control ( $\blacksquare$ ). Error bars represent standard error from two independent experiments



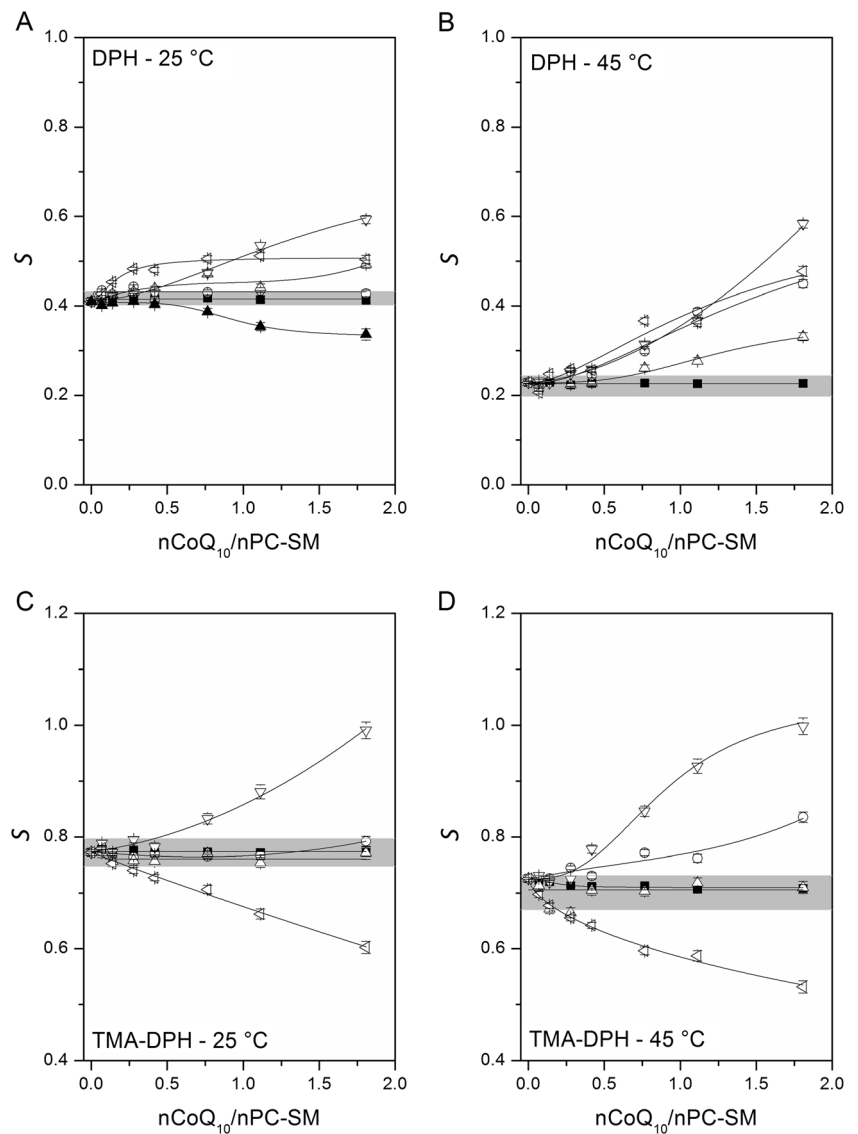
An increase in the order parameter  $S$  in the outer part of the membranes, and hence closer to the polar head groups, was detected by the fluorophore TMA-DPH for the DPPC and PC/SM SUVs when sample C was added, at both 25 and 45 °C (Fig. 3c, d; Fig. 4c, d), which contained starch sodium octenylsuccinate, dextrin and glycerol. Conversely, addition of CoQ<sub>10</sub> encapsulated in pregelatinised starch, gum arabic and lactose mixture (sample B) caused a decrease in the order parameter  $S$  (Fig. 3c, d; Fig. 4c, d). It can be speculated that the interactions of this sample B CoQ<sub>10</sub> formulation at the water–lipid interface facilitates incorporation of CoQ<sub>10</sub> into the SUV membranes, which results in the ordering of the membrane interior. However, the exact mechanism of this interaction is not known. Due to the complex compositions of the carrier systems here (with the exception of the  $\beta$ -cyclodextrin complex, as sample D), the exact mechanisms of these interactions are hard to explain at present, and further studies are needed.

### Electron Paramagnetic Resonance Spectroscopy

For the EPR spectroscopy, Fig. 5 shows the temperature dependence of the empirical correlation time ( $\tau_{emp}$ ) for the spin probes MeFASL(10,3) and MeFASL(2,11) in the PS/SM SUVs in the presence of CoQ<sub>10</sub>. With respect to the positions of the nitroxide groups, MeFASL(10,3) reports on the membrane fluidity characteristics close to the water–lipid interface, while MeFASL(2,11) reports on the changes in the middle of the bilayer [38].

These data obtained with EPR spectroscopy where the molar ratio of lipid to CoQ<sub>10</sub> was 2:1 showed smaller, but more uniform, effects of the water suspensions of the CoQ<sub>10</sub> formulations on the PC/SM SUV membranes compared to the fluorescence anisotropy measurements. When water suspensions of the CoQ<sub>10</sub> formulations were added, across the samples, effects similar to that caused by addition of the pure CoQ<sub>10</sub>

**Fig. 4** Changes in the lipid order parameter  $S$  after titration of PC/SM SUVs (molar ratio, 2.4:1) with the fluoroprobes DPH (a, b) and TMA-DPH (c, d) at 25 °C (a, c) and 45 °C (b, d). Data are shown for the water-soluble CoQ<sub>10</sub> formulations with the CoQ<sub>10</sub> concentration of 2 mg/mL, as sample A ( $\Delta$ ), sample B ( $\nabla$ ), sample C ( $\nabla$ ), and sample D ( $\circ$ ). For clarity, where the changes in the lipid order parameter  $S$  as a result of the carriers alone were located within the grey area the data are not shown, while the carriers alone for Sample A are shown (a;  $\blacktriangle$ ). Ultra pure water was used as the control ( $\blacksquare$ ). Error bars represent standard error from two independent experiments



and the on the membrane interior were detected using the spin probe MeFASL(2,11). As described previously [39] the presence of the pure CoQ<sub>10</sub>, caused a slight increase in the empirical correlation time  $\tau_{emp}$  of the spin probe MeFASL(10,3) compared to the ethanol only control over the temperature range from 15 to 35 °C (Fig. 5, inset). This effect was also more pronounced for the middle of the membranes, as revealed by the MeFASL(2,11) (Fig. 5, inset), which indicated that CoQ<sub>10</sub> promotes a decrease in the dynamics of the lipid acyl chains; i.e., it increases the ordering of membrane interior.

Similar effects were also observed when the water-soluble formulations of CoQ<sub>10</sub> were tested. There was a significant increase in the empirical correlation time  $\tau_{emp}$  (i.e., a decrease in membrane fluidity) close to the water–lipid interface (i.e., with the spin probe MeFASL(10,3)) when CoQ<sub>10</sub> encapsulated in the starch sodium octenylsuccinate dextrin and glycerol

mix was used (sample C) throughout the measured temperature range (Fig. 5). However, the effects of other samples were negligible here, except for the emulsified CoQ<sub>10</sub> formulation (sample A) where there was a decrease in the empirical correlation time  $\tau_{emp}$  at 35 and 45 °C (Fig. 5). In the middle of the membrane, as shown by the spin probe MeFASL(2,11), when the water-soluble formulations of CoQ<sub>10</sub> were used, there were increases over the control for the empirical correlation time  $\tau_{emp}$  that were similar to that caused by the pure CoQ<sub>10</sub> (Fig. 5). The main exception here was the emulsified CoQ<sub>10</sub> formulation (sample A), where there were no significant changes over the control throughout the measured temperature range (Fig. 5).

More precise descriptions of the membrane characteristics were obtained by computer simulation of the EPR spectra. As detected with MeFASL(10,3), and so in the outer part of the membranes, at temperatures below 30 °C, good fits with the



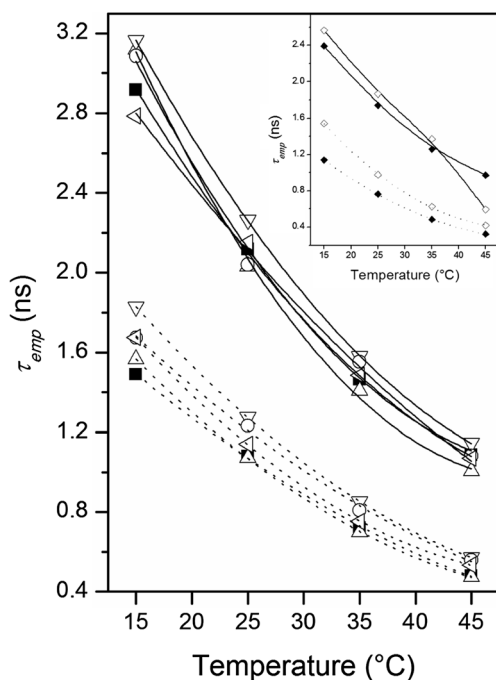


**Fig. 5** Temperature dependence of the empirical correlation time  $\tau_{emp}$  of the spin probes MeFASL(10,3) (solid lines) and MeFASL(2,11) (dotted lines) in the PS/SM SUV (molar ratio, 2.4:1) without (control, ■), and with the different water soluble CoQ<sub>10</sub> formulations, as sample A (Δ), sample B (<), sample C (∇), and sample D (○). The lipid:CoQ<sub>10</sub> ratio was 2:1. Inset: Control (◆), ethanol solution of CoQ<sub>10</sub> (◇). Measurements were performed in duplicates. The standard deviations are within the data symbols

experimental spectra were obtained according to two spectral components that described the two types of membrane regions with different fluidity characteristics that merge together at higher temperatures. The increased empirical correlation time for sample C corresponded to an increase in the order parameter  $S$  (from 0.36 to 0.41) and an increased proportion of the more ordered domain at 25 °C (from 0.47 to 0.62). With increasing temperature, the order parameter  $S$  and the proportion of the more ordered domain decreased, and at 45 °C the increase in the order parameter  $S$  compared to control was minimal (from 0.19 to 0.21) (Supplementary Fig. 1).

These differences were more pronounced in the middle of the membrane, as detected using the MeFASL(2,11) (Supplementary Fig. 2). Here, the differences in the empirical correlation time  $\tau_{emp}$  were expressed as increases in the rotational correlation time  $\tau_c$  of the less-ordered domain when these water-soluble formulations of CoQ<sub>10</sub> were present (Supplementary Table 1). These differences were most pronounced in the presence of the CoQ<sub>10</sub> encapsulated in the sodium starch octenyl succinate, dextrin and glycerol mix (sample C), followed by CoQ<sub>10</sub> in  $\beta$ -cyclodextrin (sample D), CoQ<sub>10</sub> in the pregelatinised starch, gum arabic and lactose mix (sample B), and finally the emulsified CoQ<sub>10</sub> (sample A). Interestingly, the addition of these water-soluble formulations of CoQ<sub>10</sub> and the pure CoQ<sub>10</sub> caused decreases in the polarity

correction factor of the hyperfine coupling tensor ( $p_A$ ) of both the more ordered and the less ordered domains (Supplementary Fig. 3), which suggested that the CoQ<sub>10</sub> prevented the entry of water into the membranes.

Larger deviations in the data were obtained with the fluorescence anisotropy measurements and the EPR measurements, primarily in the measurement of the changes in the water–lipid interface of the PC/SM SUV membranes. These were probably a result of differences in the shapes and dimensions of the probes used in these methods.

### Energetic Impact of CoQ<sub>10</sub> and Carriers in the CoQ<sub>10</sub> Water-Soluble Formulations on the DPPC Gel-to-Liquid Phase Transition

From the DSC measurements on the multilamellar liposomes, the changes in the enthalpy and the temperatures of the phase transitions of the lipids from the gel-to-liquid-crystalline state can be determined.

It should be stressed here that only pure lipid systems of saturated fatty acids have sharp phase transitions that can be easily determined across a narrow temperature interval [40]. In SUV suspensions that are composed of mixtures of different lipids (e.g., PC/SM in the molar ratio of 2.4:1), phase transitions cannot be determined in the temperature range from 0 to 100 °C using DSC. This is the reason why in these DSC studies the DPPC multilamellar liposomes were used [41].

The thermodynamic values of the phase transitions of the DPPC multilamellar liposomes for the full range of the samples tested are given in the Supplementary Table 2. With the addition of the CoQ<sub>10</sub> formulation where pregelatinised starch, gum arabic and lactose (sample B), starch sodium octenylsuccinate, dextrin and glycerol (sample C), and  $\beta$ -cyclodextrin (sample D) were used as carriers, an additional peak that corresponded to CoQ<sub>10</sub> aggregates in the lipid bilayer [42], was observed at  $48.1 \pm 0.1$  °C (sample B),  $49.1 \pm 0.1$  °C (sample C), and  $47.2 \pm 0.1$  °C (sample D). This effect was not observed when the carriers in these two samples were added to the DPPC multilamellar liposomes in the amount present in the samples, when the molar ratio of DPPC:CoQ<sub>10</sub> was 1:1. The amount of CoQ<sub>10</sub> that entered the DPPC bilayer was greatest when the CoQ<sub>10</sub> encapsulated in pregelatinised starch, gum arabic and lactose (sample B) was added, followed by CoQ<sub>10</sub> in  $\beta$ -cyclodextrin (sample D), and the CoQ<sub>10</sub> formulation with starch sodium octenylsuccinate, dextrin and glycerol as carriers (sample C). Since the CoQ<sub>10</sub> fraction in an aggregated state increased in proportion to its concentration in the DPPC multilamellar liposomes [39, 43], these data confirm that the carrier systems facilitate the incorporation of CoQ<sub>10</sub> into the lipid membranes, and that the composition of the carrier system affects the efficiency of the CoQ<sub>10</sub> incorporation (Supplementary Fig. 4).

Addition of the CoQ<sub>10</sub> emulsion (sample A) resulted in the disappearance of the phase pretransition  $T_m$  and a decrease in  $\Delta H_{cal}$ , the enthalpy of the gel-to-liquid crystalline transition, from  $35.5 \pm 0.5$  kJ/molK to  $29.1 \pm 0.5$  kJ/molK. This can be expected based on the composition of the carrier system of sample A, with the PGE emulsifier, glycerol and soybean lecithin. This combination resulted in an increase in the membrane fluidity.

### Evaluation of the Inhibition of Lipid Peroxidation

To access the prevention of lipid peroxidation of these water-soluble CoQ<sub>10</sub> formulations, the lipophilic fluorogenic probe BODIPY® 581/591 C<sub>11</sub> was used. The presence of pure CoQ<sub>10</sub> and of the water-soluble CoQ<sub>10</sub> formulations inhibited lipid peroxidation to different degrees. This inhibition was the greatest with sample B, which contained pregelatinised starch, gum arabic and lactose as carriers, followed by sample D and then sample C. In the presence of the emulsified CoQ<sub>10</sub> formulation (sample A), the oxidation increased exponentially after 60 min (Fig. 6). The reason for this accelerated oxidation was the presence of the unsaturated lipids (i.e., soybean lecithin) in the sample itself. The water-soluble CoQ<sub>10</sub> formulations inhibited the lipid oxidation to a greater degree than the pure CoQ<sub>10</sub>, which suggested that the encapsulation of CoQ<sub>10</sub> into these different carrier systems allows better dispersion of the CoQ<sub>10</sub> in water. Lipid membrane–CoQ<sub>10</sub> interactions are facilitated, which provides better protection from oxidation.

### Conclusions

The aim of this study was to better understand the effects of carriers on the interactions between water-soluble CoQ<sub>10</sub>

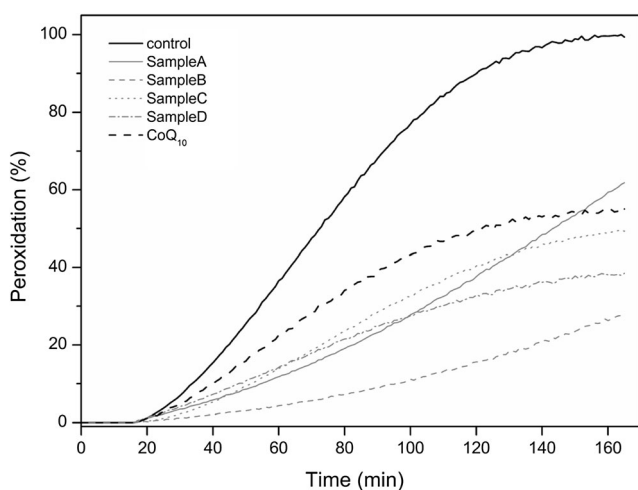


**Fig. 6** Inhibition of peroxidation of egg phosphatidylcholine induced by CuCl<sub>2</sub> in the presence of the different water-soluble CoQ<sub>10</sub> formulations (10 mol%), measured as the fluorescence emission from BODIPY® 581/591 C<sub>11</sub>

formulations and model lipid membranes. These data show that the pure CoQ<sub>10</sub> and the majority of the water soluble CoQ<sub>10</sub> formulations investigated here (which can be found in food supplements) resulted in a decrease of the membrane fluidity that was more pronounced in the middle of the membranes, thus indicating that the CoQ<sub>10</sub> penetrates into the membrane.

Fluorescence anisotropy and EPR data showed increased lipid ordering within the region occupied by the fatty acid residues suggesting that the CoQ<sub>10</sub> is located within this region. Our data agrees with the findings of Grzybek et al. [44] and Hauss et al. [45], reporting larger effect of CoQ<sub>10</sub> on the interior of the membrane bilayer. Penetration of CoQ<sub>10</sub> into the membrane interior was additionally confirmed by DSC. The appearance of a new peak in the thermogram corresponded to CoQ<sub>10</sub> aggregates in the lipid bilayer as reported by Katsikas and Quinn [42].

With the exception of the carriers in the emulsified formulation of CoQ<sub>10</sub> (sample A), the samples with the carriers alone did not have any significant effects on the membrane properties, which showed that the changes in the membranes were caused by the CoQ<sub>10</sub>. In addition, the water-soluble CoQ<sub>10</sub> formulations provided better protection from lipid peroxidation in the liposome solutions, showing better perturbation of the water-soluble CoQ<sub>10</sub> formulations into the lipid membrane, than for the pure CoQ<sub>10</sub>.

These data obtained with fluorescence spectroscopy, EPR spectroscopy and DSC show that the commercially available formulation of CoQ<sub>10</sub> with starch sodium octenylsuccinate, dextrin and glycerol as carriers (sample C) was the best delivery system for CoQ<sub>10</sub> in these lipid membranes.

Our study also shows that the lipid composition of the membranes influences their interactions with CoQ<sub>10</sub>. Due to the complex composition of the carrier systems of the samples studied here, the exact mechanisms of these interactions remain hard to explain at this stage. Further studies will help in the understanding and improving of the encapsulation of CoQ<sub>10</sub> for its better delivery and bioavailability.

**Acknowledgments** This study was supported by the Slovenian Research Agency (ARRS) through the programme P4-012 (N.P.U.), and by the European Social Fund of the European Union (A.O.).

### References

1. B. Frei, M.C. Kim, B.N. Ames, P. Nat. Acad. Sci. U.S.A. **87**, 4879–4883 (1990)
2. H.N. Bhagavan, R.K. Chopra, Free Radic. Res. **40**, 445–453 (2006)
3. C. Schulz, U.C. Obermuller-Jevic, O. Hasselwander, J. Bernhardt, H.K. Biesalski, Int. J. Food Sci. Nutr. **57**, 546–555 (2006)
4. M.V. Bule, R.S. Singhal, J.F. Kennedy, Carbohydr. Polym. **82**, 1290–1296 (2010)
5. B. Siekmann, K. Westesen, Pharm. Res. **12**, 201–208 (1995)

6. C.-H. Hsu, Z. Cui, R. Mumper, M. Jay, *AAPS PharmSciTech* **4**, 24–35 (2003)
7. T.R. Kommuru, B. Gurley, M.A. Khan, I.K. Reddy, *Int. J. Pharm.* **212**, 233–246 (2001)
8. H. Takeuchi, H. Sasaki, T. Niwa, T. Hino, Y. Kawashima, K. Uesugi, H. Ozawa, *Int. J. Pharm.* **86**, 25–33 (1992)
9. M. Milivojević Fir, A. Šmidovnik, L. Milivojević, J. Žmitek, M. Prošek, *J. Incl. Phenom. Macro.* **64**, 225–232 (2009)
10. I. Pravst, M. Prošek, A.G. Wondra, K. Zmitek, J. Zmitek, *Acta Chim. Slov.* **56**, 953–958 (2009)
11. B.D. Tobin, M.G. O'Sullivan, R. Hamill, J.P. Kerry, *Food Chem.* **150**, 187–192 (2014)
12. P.M.M. Schroyen, R. van der Meer, C.G. De Kruif, *Proc. Nutr. Soc.* **60**, 475–479 (2001)
13. T.A. Reineccius, G.A. Reineccius, T.L. Peppard, *J. Food Sci.* **67**, 3271–3279 (2002)
14. G.A. Reineccius, *Dry. Technol.* **22**, 1289–1324 (2004)
15. A. Madene, M. Jacquot, J. Scher, S. Desobry, *Int. J. Food Sci. Technol.* **41**, 1–21 (2006)
16. L. Szente, J. Szejtli, *Trends Food Sci. Technol.* **15**, 137–142 (2004)
17. T. Bhardwaj, M. Kanwar, R. Lal, A. Gupta, *Drug Dev. Ind. Pharm.* **26**, 1025–1038 (2000)
18. A.V. Reis, M.R. Guilherme, T.A. Moia, L.H.C. Mattoso, E.C. Muniz, E.B. Tambourgi, *J. Polym. Sci. Pol. Chem.* **46**, 2567–2574 (2008)
19. C. Peetla, A. Stine, V. Labhasetwar, *Mol. Pharm.* **6**, 1264–1276 (2009)
20. D.D. Lasic, *Liposomes: from physics to applications* (Elsevier, 1993), p 575
21. M. Šentjurc, K. Vrhovnik, J. Kristl, *J. Control. Release* **59**, 87–97 (1999)
22. H. Pottel, W. Vandermeer, W. Herreman, *Biochim. Biophys. Acta* **730**, 181–186 (1983)
23. A. Ota, D. Gmajner, M. Sentjurc, N.P. Ulrih, *Archaea*, 1–9 (2012)
24. D. Marsh, in *Membrane Spectroscopy*, ed. By E. Grell (Springer Berlin Heidelberg, 1981), pp. 51–142
25. L. Coderch, J. Fonollosa, J. Estelrich, A. De La Maza, J.L. Parra, *J. Control. Release* **68**, 85–95 (2000)
26. V. Abram, B. Berlec, A. Ota, M. Sentjurc, P. Blatnik, N.P. Ulrih, *Food Chem.* **139**, 804–813 (2013)
27. D. Gmajner, A. Ota, M. Sentjurc, N.P. Ulrih, *Chem. Phys. Lipids* **164**, 236–245 (2011)
28. J. Strancar, T. Koklic, Z. Arsov, *J. Membr. Biol.* **196**, 135–146 (2003)
29. J. Strancar, T. Koklic, Z. Arsov, B. Filipic, D. Stopar, M.A. Hemminga, *J. Chem Inf. Model.* **45**, 394–406 (2005)
30. Z. Arsov, J. Štrancar, *J. Chem. Inf. Model.* **45**, 1662–1671 (2005)
31. M.E. Johnson, D.A. Berk, D. Blankschtein, D.E. Golan, R.K. Jain, R.S. Langer, *Biophys. J.* **71**, 2656–2668 (1996)
32. A. Ota, H. Abramovic, V. Abram, N.P. Ulrih, *Food Chem.* **125**, 1256–1261 (2011)
33. G.P.C. Drummen, L.C.M. van Liebergen, J.A.F. Op den Kamp, J.A. Post, *Free Radic. Biol. Med.* **33**, 473–490 (2002)
34. J.R. Lakowicz, *Principles of Fluorescence Spectroscopy*, 3rd edn. (Springer London, Limited, 2006)
35. X.L. Xu, E. London, *Biochem.-U.S.* **39**, 843–849 (2000)
36. M. JemiolaRzeminska, J. Kruk, M. Skowronek, K. Strzalka, *Chem. Phys. Lipids* **79**, 55–63 (1996)
37. B. McCormack, G. Gregoriadis, *Int. J. Pharm.* **112**, 249–258 (1994)
38. W.K. Subczynski, A. Wisniewska, J.J. Yin, J.S. Hyde, A. Kusumi, *Biochem.-U.S.* **33**, 7670–7681 (1994)
39. A. Ota, M. Sentjurc, N.P. Ulrih, *Int. J. Membr. Sci. Tech.* **2**, 34–38 (2015)
40. M. Budai, Z. Szabo, M. Szogyi, P. Grof, *Int. J. Pharm.* **250**, 239–250 (2003)
41. B. Pawlikowska-Pawlega, W.I. Gruszecki, L.E. Misiak, A. Gawron, *Biochem. Pharmacol.* **66**, 605–612 (2003)
42. H. Katsikas, P.J. Quinn, *FEBS Lett.* **133**, 230–234 (1981)
43. E.L. Ulrich, M.E. Girvin, W.A. Cramer, J.L. Markley, *Biochem.-U.S.* **24**, 2501–2508 (1985)
44. M. Grzybek, K. Stebelska, P. Wyrozutnska, et al., *Gen. Physiol. Biophys.* **24**(4), 449–460 (2005)
45. T. Hauss, S. Dante, T. H. Haines and N. A. Dencher, *Biochim Et Biophys Acta-Bioenergetics* 1710 (1), 57–62 (2005)